International Journal of Pharmaceutics 626 (2022) 122135

Contents lists available at ScienceDirect

International Journal of Pharmaceutics

journal homepage: www.elsevier.com/locate/ijpharm

Personalised paediatric chewable Ibuprofen tablets fabricated using 3D micro-extrusion printing technology

Atabak Ghanizadeh Tabriz [a,c], Uttom Nandi [a,c], Nicolaos Scoutaris [a,c], Karifa Sanfo [a], Bruce Alexander [a], Yuchuan Gong [b], Ho-Wah Hui [b], Sumit Kumar [b,*], Dennis Douroumis [a,c,1,*]

[a] Faculty of Engineering and Science, School of Science, University of Greenwich, Chatham Maritime, Chatham, Kent ME4 4TB, UK
[b] Drug Product Development, Bristol Myers Squibb (formerly Celgene Corporation), 556 Morris Avenue, Summit, NJ 07901, USA
[c] CIPER Centre for Innovation and Process Engineering Research, Kent ME4 4TB, UK

ARTICLE INFO

Keywords:
3D printing
Personalized
Paediatric
Micro-extrusion
Taste masking
Raman mapping

ABSTRACT

Three-dimensional (3D) printing is becoming an attractive technology for the design and development of personalized paediatric dosage forms with improved palatability. In this work micro-extrusion based printing was implemented for the fabrication of chewable paediatric ibuprofen (IBU) tablets by assessing a range of front runner polymers in taste masking. Due to the drug-polymer miscibility and the IBU plasticization effect, micro-extrusion was proved to be an ideal technology for processing the drug/polymer powder blends for the printing of paediatric dosage forms. The printed tablets presented high printing quality with reproducible layer thickness and a smooth surface. Due to the drug-polymer interactions induced during printing processing, IBU was found to form a glass solution confirmed by differential calorimetry (DSC) while H-bonding interactions were identified by confocal Raman mapping. IBU was also found to be uniformly distributed within the polymer matrices at molecular level. The tablet palatability was assessed by panellists and revealed excellent taste masking of the IBU's bitter taste. Overall micro-extrusion demonstrated promising processing capabilities of powder blends for rapid printing and development of personalised dosage forms.

1. Introduction

Three-dimensional (3D) printing, as an evolving technology, has attracted a great deal of attention in various medical fields, particularly in drug delivery, such as fabrication of solid dosages forms (Scoutaris et al., 2018), films (Hafezi et al., 2019), and microneedles (Pere et al., 2018). Within the past decade, a significant number of published research have exploited 3D additive applications for the design and printing of novel drug delivery systems (Goyanes et al., 2015b; Scoutaris et al., 2016; Trenfield et al., 2018; Zhu et al., 2020). These studies have shown that the drug release can be tailored to each specific patient's need by adjusting the tablet design and the selection of compatible pharma grade polymers for 3D printing.

The most widely used 3D printing technologies include fused deposition modelling (FDM), selective laser sintering (SLS), stereolithography, and inkjet printing. Most of the 3D printing technologies are compatible with pharma grade polymers which makes 3D printing an attractive and alternative approach for the fabrication of solid dosage forms in particular for personalised medicine.

A distinctive advantage of FDM technology in comparison with other 3D printing technologies is it's compatibility of majority of pharma grade polymers such as hydroxypropyl methylcellulose (HPMC) (Kadry et al., 2018), hydroxypropyl methylcellulose acetate succinate (Goyanes et al., 2017), Ethyl cellulous (Yang et al., 2018) and Hydroxypropyl cellulose (Chai et al., 2017). FDM has been proved to be a versatile 3D printing technology in fabricating personalised medicines. Using the technology, tablets were printed with unique designs that resulted in modified drug release profiles (Goyanes et al., 2015a; Jamróz et al., 2018). Polypills (Pereira et al., 2019) and bilayer solid dosage forms (Ghanizadeh Tabriz et al., 2020; Gioumouxouzis et al., 2018) were also printed using FDM to improve patient's compliance (Castellano et al., 2014).

SLS has also seen its application in fabrication of solid dosage forms. Fina et. al. studied the printability of several pharmaceutical grade polymers such as Eudragit, polyethylene oxide and ethyl cellulose using SLS technology (Fina et al., 2018, 2017). Wang et al. (2016) investigated

* Corresponding authors.
E-mail addresses: yuchuangong@gmail.com (Y. Gong), sumit_kum@outlook.com (S. Kumar), D.Douroumis@gre.ac.uk (D. Douroumis).
[1] Pharmaceutical Technology and Process Engineering, Chatham Maritime, Chatham, Kent ME4 4TB, UK.

https://doi.org/10.1016/j.ijpharm.2022.122135
Received 9 June 2022; Received in revised form 3 August 2022; Accepted 18 August 2022
Available online 24 August 2022

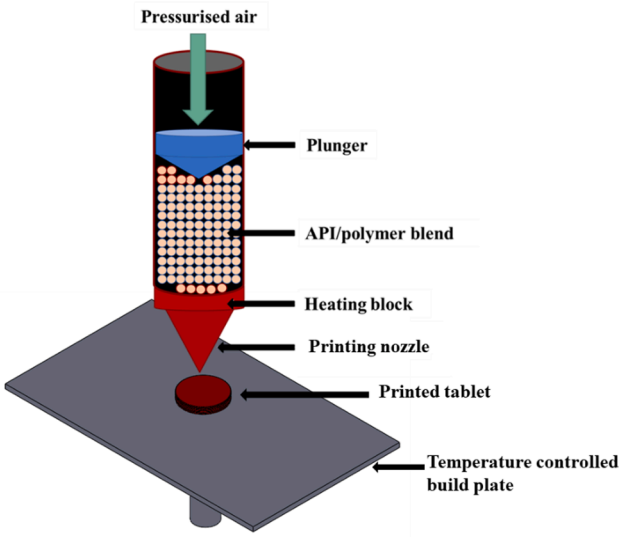

Fig. 1. Schematic drawing of micro-extrusion printhead for tablet printing.

the suitability of SLS technology in fabricating PEGDA/paracetamol tablets. Martinez et al. (2018) showed SLS may be used to fabricate drug loaded tablets with modified release by altering the tablet geometry.

Inkjet printing has also shown its potential for the fabrication of solid dosage forms despite there is limited choice of compatible polymers. A study by Kyobula et al. (2017) showed inkjet printing may be used for fabrication of tablets using an FDA approved beeswax. It was observed that drug release can be tailored based on the design of the 3D printed tablets.

All the above-mentioned 3D printing technologies require powders to be pre-processed before 3D printed into tablets, which may limit the choice of pharma grade polymers. FDM printing technology exclusively uses hot melt extrusion as the pre-process to generate drug loaded filaments. Rheological behaviour (Elbadawi et al., 2020) and mechanical properties (Nasereddin et al., 2018; Öblom et al., 2019; Xu et al., 2020; Zhang et al., 2017) of certain materials may limit their application in 3D printing using FDM technology. SLA technology requires developing drug loaded photocurable resins, which also limits of the choices of pharma grade polymers that can be used. In addition, SLS technology provides less control over the tablet design in comparison to FDM, which may limit its applications in drug delivery systems. Inkjet printing requires materials with low viscosity, which makes it less applicable in fabricating solid dosage forms containing pharma grade polymers. Nevertheless, a direct powder extrusion technology has been reported by other researchers to overcome pitfalls of existing 3D printing technologies (Boniatti et al., 2021; Goyanes et al., 2019). In this approach, pellets or milled extrudates can be processed with a with a direct powder extruder nozzle for the printing of the designed dosage forms. The technology has found applications for the development of praziquantel paediatric dosage forms and personalised dosage forms.

3D printing technologies have been implemented for the development of paediatric dosage forms over the past five years (Januskaite et al., 2020). The first study was conducted by Scoutaris et al. (2018) by fabricating "candy-like" formulations imitating Starmix confectionaries. The extruded filaments comprised of indomethacin and hypromellose acetate succinate effectively masked the bitter taste of the drug. Rycerz et al. (2019) used semi-solid gelatin-based inks to print Lego™ like chewable tablets containing paracetamol and ibuprofen. Recently Wang et al. (2020) 3D printed donut-shaped tablets containing caffeine citrate. By adjusting the infill density, the authors prepared paediatric immediate release dosage forms with efficient taste masking. Tagami et al. (2021) prepared 3D printed gummy drug formulation comprising of gelatin, HPMC, syrup, water, and lamotrigine that had 85% drug release within 15 min.

The aim of this study was to introduce a novel micro-extrusion 3D printing approach that does not require pre-processing steps while still allows control of drug release by tablet design. The technology was used to develop personalised chewable paediatric tablets with good palatability. The physiochemical properties of the 3D printed tablets were also determined to evaluate the potential application of the technology in developing personalised paediatric medication.

2. Materials and methods

2.1. Materials

Soluplus (SOL) and PVP VA-64 (VA64) were kindly donated by BASF (BASF-Germany). Eudragit EPO (EPO) was kindly donated by Evonik (Evonik-Germany). Ibuprofen (IBU) was purchased from IOL Chemicals and Pharmaceuticals Ltd (Punjab, India).

2.2. Formulation preparation

PVP-VA64, EPO or Soluplus were blended with Ibuprofen at a ratio of 60/40 (w/w) using a turbula shaker-mixer (Glen Mills T2F Shaker/Mixer, USA) at 100 rpm for ten minutes. Tablets were prepared with each blend using micro-extrusion technology.

2.3. Thermal gravimetric analysis (TGA)

TGA technique (TGA Q5000 Thermal instruments, USA) was utilised to investigate the thermal stability of bulk polymers and Ibuprofen. 2–2.5 mg of polymer and drug samples were carefully weighed and positioned in to a standard 40 μL aluminium pan. The samples were heated from 25 °C to 500 °C at 10 °C/min. The extracted raw data were analysed via TA Universal Analysis software (Universal Analysis 2000, version 4.5A, TA instruments, USA).

2.4. Differential scanning calorimetry (DSC)

Differential scanning calorimeter (Mettler-Toledo 823e, Switzerland) was utilised to investigate the thermal behaviour of bulk materials and 3D printed tablets as well as for investigation of physical state of the Ibuprofen within the 3D printed tablets. bulk materials and a small portion of the 3D printed tablets were approximately weighed between 2 and 2.5 mg and located into a 40 μ L aluminium pan and crimped promptly. The bulk polymer and 3D printed samples were heated from 25 °C to 160 °C at a rate of 10 °C/min. Ibuprofen was heated from 25 °C to 120 °C at a rate of 10 °C/min. The extracted DSC thermograms of bulk materials and the 3D printed tablets were analysed through STARe Excellence Thermal Analysis Software (Mettler Toledo, Switzerland).

2.5. Design and 3D printing of Ibuprofen tablets

Two tablet designs were constructed to investigate the micro extrusion (printability) of various polymer/IBU formulations. The tablets were designed via SolidWorks software (Dassault Systems, USA) and converted into (stereolithography) stl files. Both tablets have the same diameter of 12 mm but different heights, (i.e., 3 mm or 2.4 mm) and were sliced with 40% and 60 % infill density, respectively. The infill densities were designed in a manner to have a total weight of 250 mg comprising 100 mg of ibuprofen. A Bio-X (Celink, Sweden) bioprinter with a pneumatic thermoplastic printhead was used to 3D print the tablets. Approximate 3 g of each blend were placed into a heat-able metallic reservoir and the tablets were printed using a 0.4 mm nozzle, 0.4 mm layer height and 5 mm/s print speed.

The printing temperature for IBU/VA64, IBU/EPO and IBU/Soluplus was set to 120 °C, 90 °C and 105 °C respectively. The respective

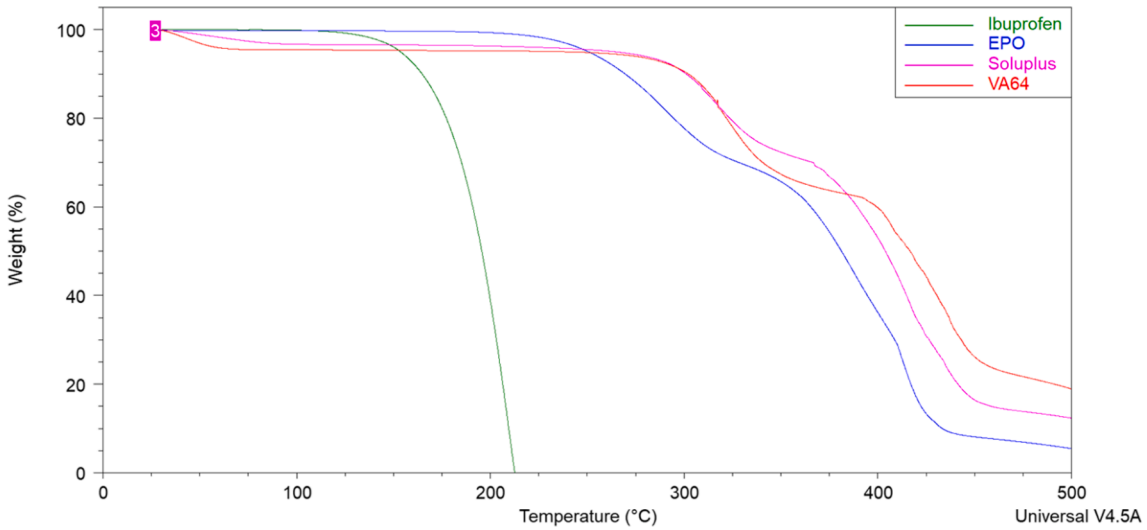

Fig. 2. TGA graphs of the bulk EPO, Soluplus, VA64 and Ibuprofen.

pneumatic pressure used for the formulations was set at 120 kPa, 110 kPa and 90 kPa while the build plate temperature was maintained at 15 °C. As shown in Fig. 1, the schematic drawing of micro-extrusion process of the tablets represents that a pressurised air pushes a metallic plunger towards the physical blend within the reservoir by coordinating the horizontal movement of the printhead and the vertical movement of the printhead where tablet designs with different infill densities were successfully fabricated.

2.6. Scanning electron microscopy (SEM)

Scanning electron microscopy (Hitachi SU8030, Japan) was utilised to investigate the quality/layer height of the printed tablets via micro-extrusion. Tablets were kept secured on an aluminium stub with a conductive carbon adhesive tape (Agar Scientific, Stansted, UK). The tablets were then examined via SEM and images were captured by an electron beam accelerating voltage of 1KV and magnification of 30x.

2.7. X-Ray powder diffraction (XRPD)

The physical state of the plain polymers, Ibuprofen and the 3D printed tablets (VA64/IBU, EPO/BU and Soluplus/IBU were investigated via XRPD. XRPD data were collected using a D8 Advance X-ray Diffractometer (Bruker AXS, Germany) equipped with a LynxEye silicon strip position sensitive detector and parallel beam optics. The diffractometer was operated with transmission geometry using Cu Kα radiation at 40 kV and 40 mA. The instrument was computer controlled using XRD commander software (Version 2.6.1, Bruker AXS, Germany) and the data was analysed using the EVA software (version 5.2.0.3, Bruker AXS, Germany). Samples were placed between foils of 2.5 μm thick mylar for measurement. Data was collected between 5 and 60° 2θ with a step size of 0.04° and a counting time of 0.2 s per step.

2.8. In vitro dissolution studies

In vitro dissolution studies were carried out to investigate the API release in acidic and neutral media for the 3D printed ibuprofen tablets. Drug release studies were carried out using a Varian 705 DS (USA) dissolution bath, attached with a paddle apparatus. Experiments were done at 37 ± 1 °C using 900 mL of 0.1 N HCl media at pH 1.2 or phosphate buffer saline (PBS, pH 7.2) in each vessel and paddles rotation were set to 50 rpm. PBS were prepared using 1.44 g disodium hydrogen phosphate, 0.24 g potassium dihydrogen phosphate and 8 g of sodium chloride (Barbero et al., 2016). Each time 2 mL of sample media were collected at 15, 30, 60, 90- and 120-minutes time interval and same amount of fresh PBS media were also added to maintain a constant volume of dissolution media. Collected samples were filtered using a 0.45 μm disk filter and poured into the High-performance liquid chromatography vial for ibuprofen concentration analysis. This study was done using an Agilent 1200 series HPLC system equipped with a gradient elution system, an autosampler, HICHROM S5ODS2-4889 (5 × 150 × 4 mm) column and an UV detector set at a wavelength of 214 nm. Samples were eluted using a mobile phase consisted of acetonitrile: water: Orthophosphoric acid (49.5: 49.3: 0.2 v/v) and pumped at a flow rate of 1.5 mL/min. Such specifications showed approximately 115 bar of column back pressure with a retention time of 3 min. Calibration curve was also prepared using IBU in HPLC grade methanol at a concentration of 10, 20, 30, 40 and 50 μg/mL. All the experiments were studied in triplicates using the same method mentioned above.

2.9. Taste masking

In vivo taste masking investigation was caried out on 10 healthy human volunteers from whom informed consent was first obtained (approved by the Ethics Committee of the University of Greenwich). The study is also in accordance with the Code of Ethics of the World Medical Association (Declaration of Helsinki). The age category of the volunteers (either sex) was selected from a 18–30. The volunteers were trained and examined the bulk substance and the 3D printed tablets orally in the mouth for 2 min and spat out promptly. No substance and tablet were swallowed, and the mouth was rinsed immediately after the experiment. The bitterness of the bulk substances and the 3D printed tablets were recorded from an intensity scale of 1 to 5 where 1, 2, 3, 4, and 5 indicate no, threshold, slight, moderate, and strong bitterness respectively.

2.10. Raman spectra and mapping

The IBU-based samples and its excipients were analysed using a Horiba LabRam I microscope fitted with a frequency-doubled Nd:YAG laser (λ = 532 nm) with a 50 times long-working distance objective. Spectra of the IBU/EPO tablet and EPO polymer were recorded with a laser power of 25%, 8 accumulations at 1 s accumulation time; meanwhile a laser power of 25%, 4 accumulations at 2 s accumulations time was utilised for the remaining spectra. Finally, maps were generated over a 120 × 180 μm area with spectra acquired every 20 μm.

Raman mapping was performed covering an area of 160 × 120 μm^2 in a recorded of 20 × 20 spectra in × and y for IBU/EPO and IBU/SOL samples while for IBU/VA64 33 × 25. The spectra were initially baseline

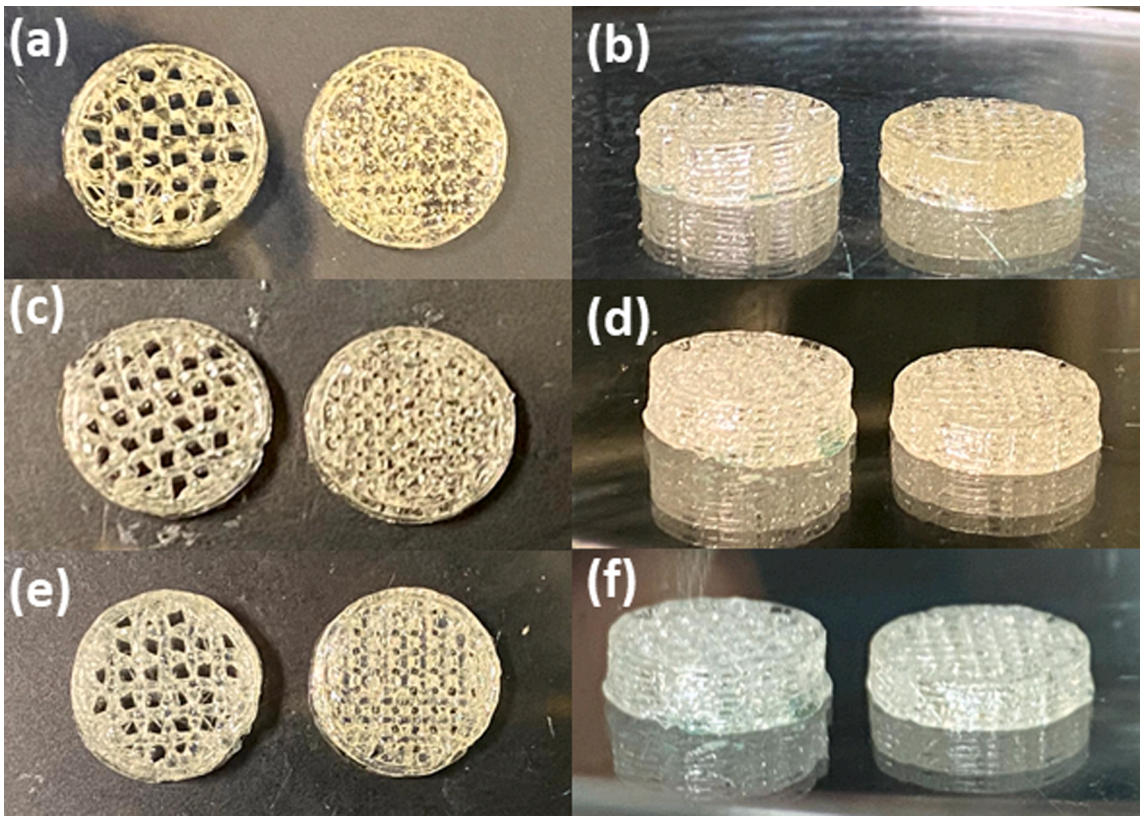

Fig. 3. Optical images of the 3D printed tablets based on 40% and 60% infill density. (a) EPO/IBU tablets, top view and (b) side view. (c) Soluplus/IBU tablets top and (d) side view. (e) VA64/IBU tablets top and (f) side view.

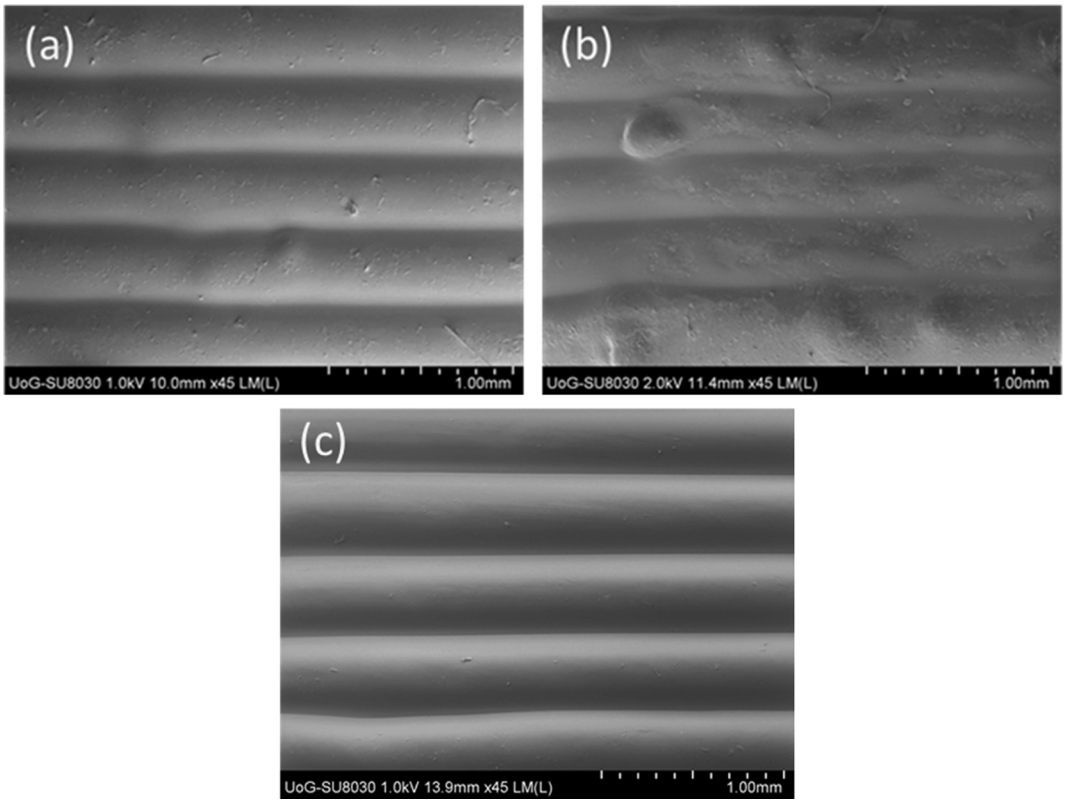

Fig. 4. SEM images of (a) EPO/IBU, (b) Soluplus/IBU and (c) VA64/IBU 3D printed tablets.

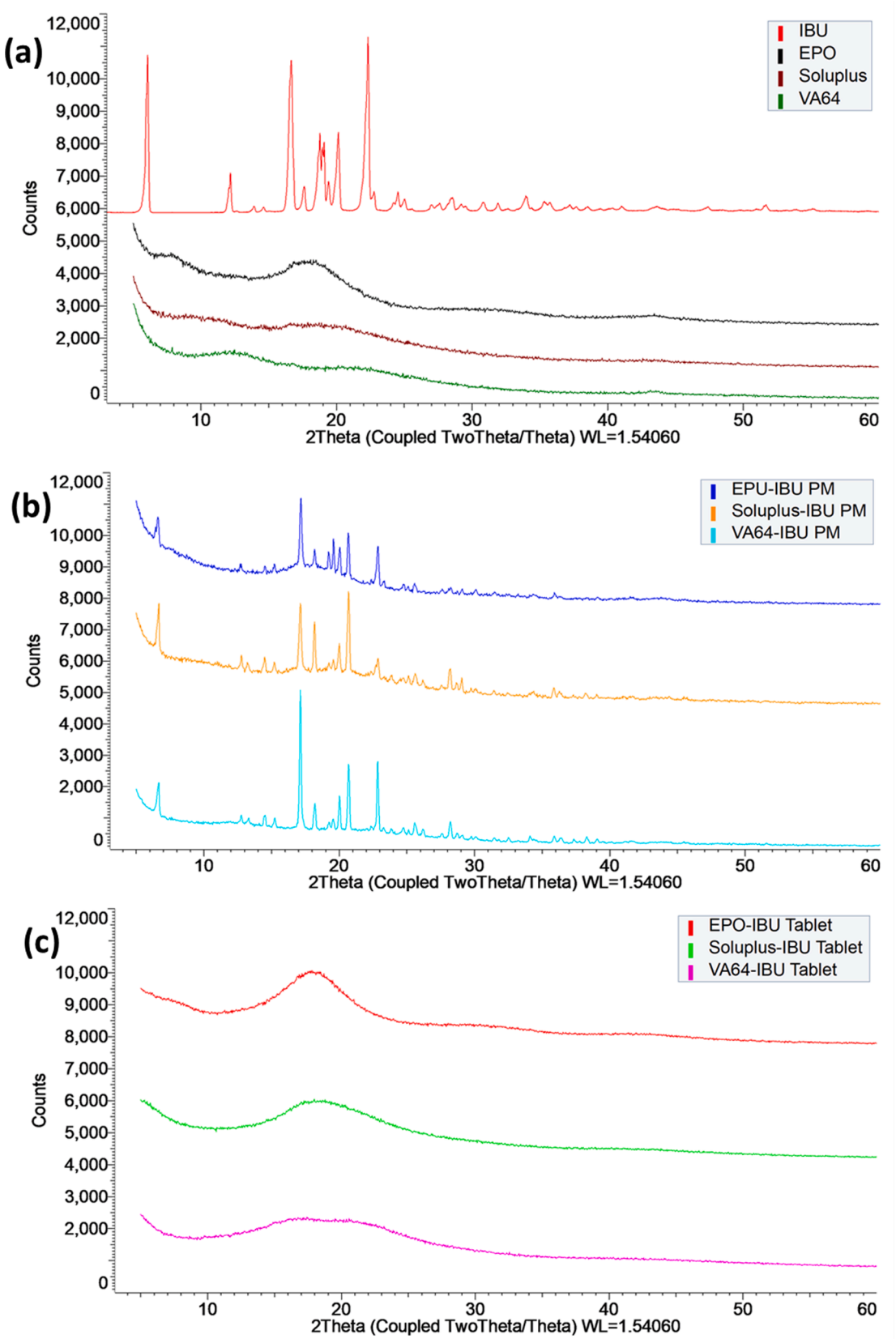

Fig. 5. XRD graphs of (a) plain EPO, Soluplus, EPO and Ibuprofen. (b) physical mixtures of IBU/polymer formulations and the (c) 3D printed tablets.

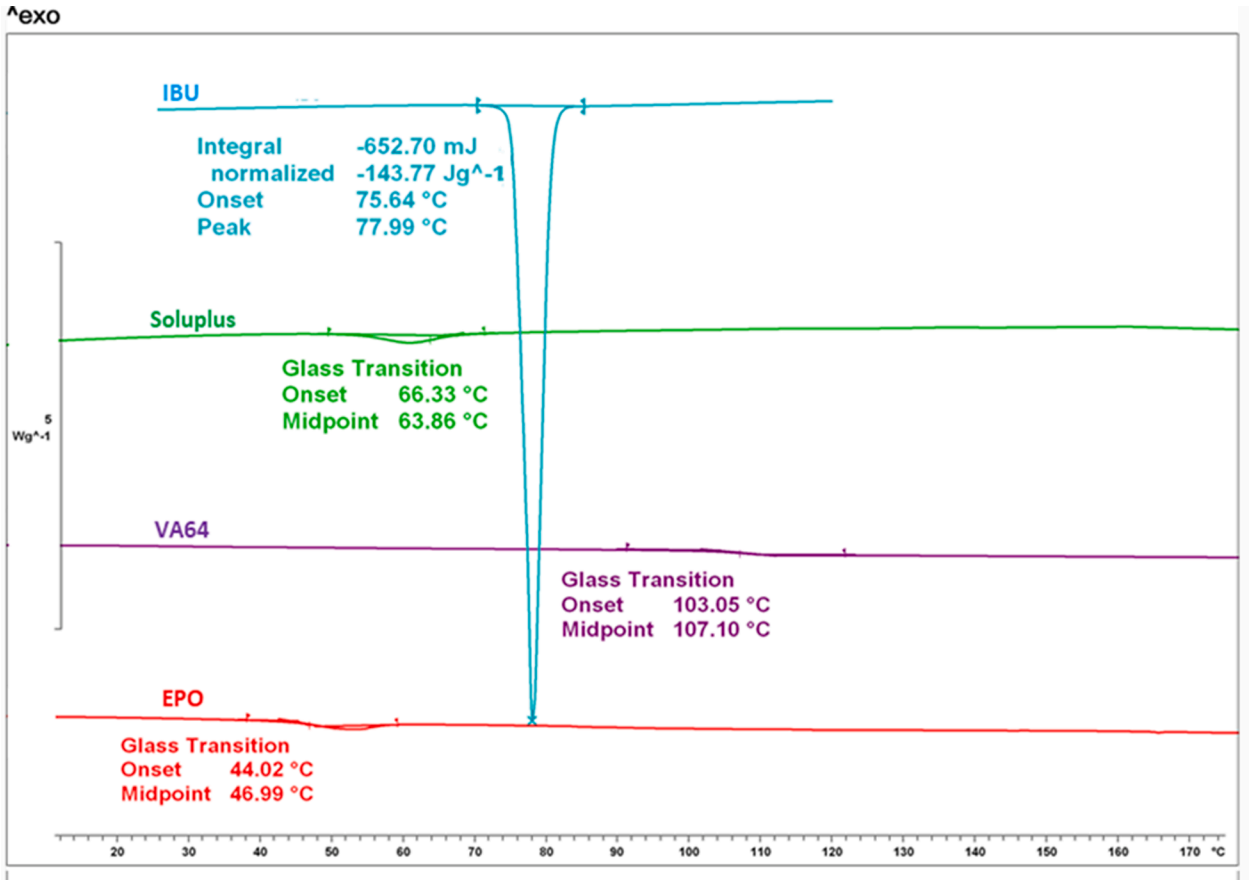

Fig. 6. DSC thermograms of bulk polymers and Ibuprofen.

corrected using the asysmetric least square (AsLS) method having as parameters lambda equal to 10^5 and p equal to 10^{-3} (Eilers and Boelens, 2005; R Core Team, 2019; Wehrens et al., 2015). In order to correct the loss of focus and scattering effect due to abnormalities in tablets' surface, the spectra were normalized using the standard normal variate. Subsequently principal component analysis used to decompose the matrix to the most prevalent factors. The analysis was caried out using R programming language (R 4.03) (R Core Team, 2019) and the ptw package to apply AsLS (Wehrens et al., 2015).

3. Results and discussion

3.1. Thermal analysis of bulk materials

In order to identify the suitable micro-extrusion temperatures, TGA analysis was carried out to evaluate the thermal stability of IBU and the bulk polymers (Fig. 2). IBU was thermally stable when it was heated up to 140 °C, beyond which the drug degraded with a rapid weight loss. Soluplus (SOL) had a gradual 4% weight loss up to 90 °C due to removal of moisture and remained stable till 260 °C beyond which the polymer degraded. PVP-VA64 (VA64) exhibited a slightly higher initial weight loss (5.5%) due to higher moisture content and did not have significant degradation till 260 °C. Eudragit EPO (EPO) remained stable with no weight loss up to 220 °C followed by a rapid loss due to the polymer degradation.

DSC thermal analysis was also carried out to characterize the thermal properties of IBU and the bulk polymers (Fig. 6). IBU, as a crystalline solid, exhibited a sharp melting endotherm at 77.99 °C. The bulk polymers, SOL, VA64, and EPO, exhibited glass transition temperature (T_g) at 66.33 °C, 107.10 °C, and 46.99 °C, respectively. The change of heat capacity at the glass transition temperatures confirmed the amorphous nature of the polymers.

The operating temperature for the micro-extrusion should be maintained below the degradation temperature of each component. In addition, the drug/polymer blends may be processed around the glass transition temperatures of the polymers to facilitate the mixing of the drug and polymers. Therefore, 3D printing of IBU/SOL, IBU/VA64, and IBU/EPO powder was carried out at 62.0 °C, 105.0 °C, and 46 °C, respectively.

3.2. Tablet design and 3D printing

Blends were printed into tablets with the same diameter of 10 mm and two infill densities (40% and 60%), to evaluate the printability and the impact of polymer type and infill density on the drug release. All blends had an IBU/polymer ratio of 40/60 (w/w). With a total weight of 250 mg, each tablet consisted 100 mg of IBU.

Previous studies demonstrated that VA64, SOL, and EPO were not suitable for 3D printing using FDM technology. The ductile nature of the polymers made it challenging to form filaments with the diameter and length desired for the following 3D printing (Alhijjaj et al., 2016; Fuenmayor et al., 2018; Sadia et al., 2016). High levels of plasticizers (e.g., 20–30%) had to be added to the polymers to improve their printability, which limited the maximum drug load in the final tablets.

The major advantage of micro-extrusion technology is that drug/polymer blends can be printed directly without having to fabricate filaments as a pre-step. Using this method, a drug/polymer blend, at various ratios, is molten or soften in the cartridge. The soften drug/polymer blend is then extruded/deposited through a heated nozzle by applying pneumatic pressure (20–700 kPa). The resulting thermoplastic filament can be printed directly into tablet shapes. Micro-extrusion technology, comparing to FDM and SLS, allows reduction of overall

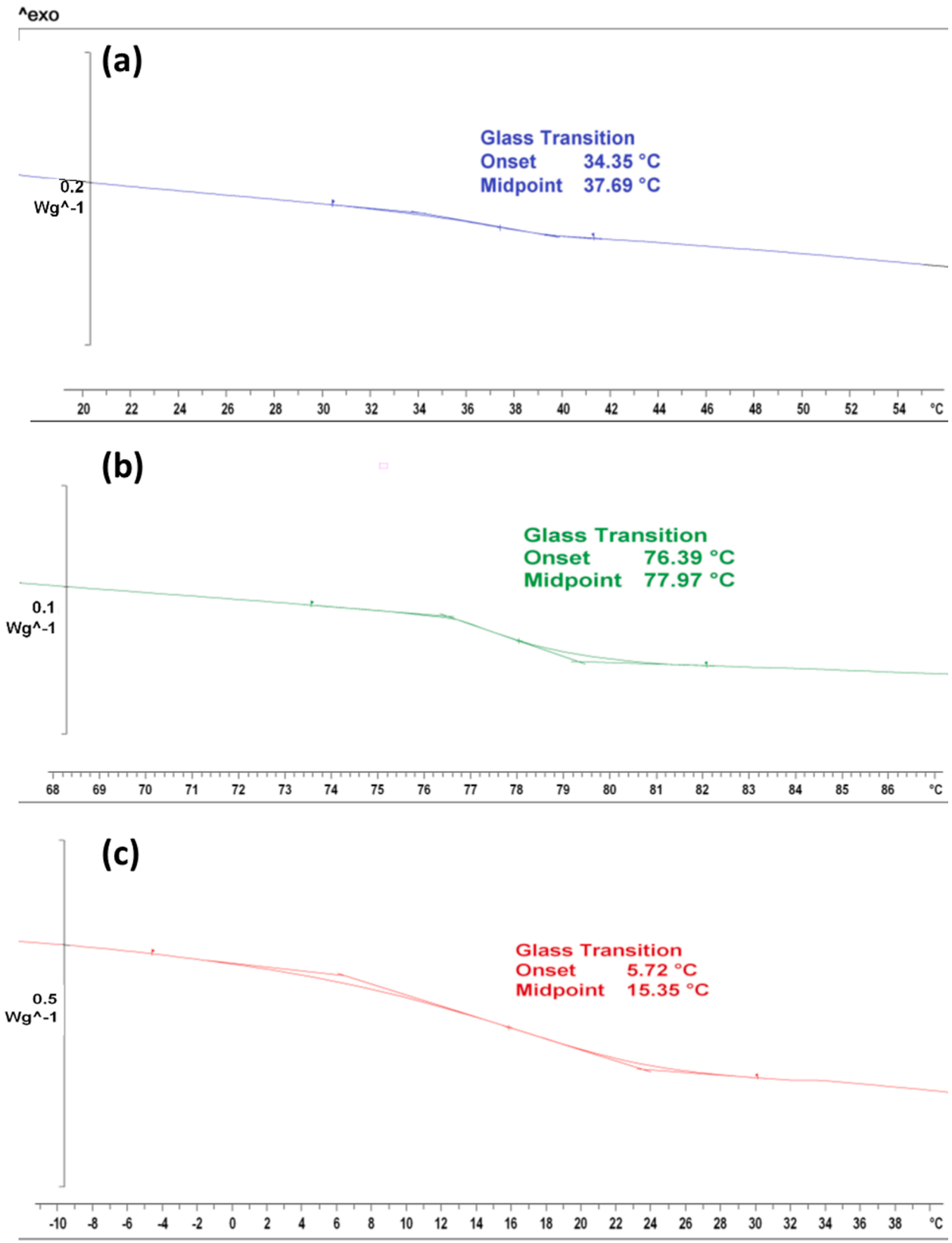

Fig. 7. Glass transition integrations of (a) Soluplus/IBU, (b) VA64/IBU and (c) EPO/IBU tablets.

processing time of 3D printing and waste of printed materials. The latter is especially valuable when making personalized medicines consisting costly API's.

As shown in Fig. 3, tablets with both infill densities were successfully fabricated with good reproducibility using micro-extrusion 3D printing technique. SEM images of the printed tablets showed consistent height of deposited layers, which demonstrated the excellent print quality of the tablets (Fig. 4).

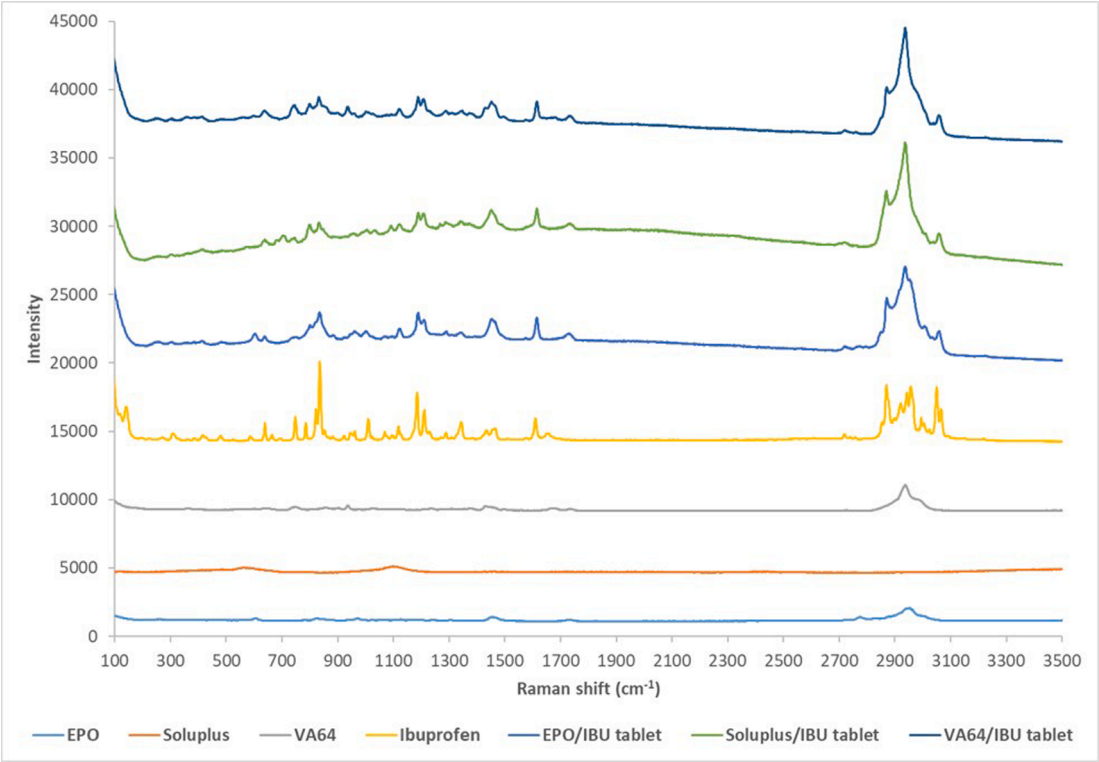

Fig. 8. Raman spectra of bulk polymers, Ibuprofen and the 3D printed Ibuprofen/polymer tablets.

The speed of 3D printing depends on the size of nozzle, printing temperature, and pneumatic pressure applied to the blend. In this study, pneumatic pressures were maintained at 90–120 kPa with a 0.4 mm nozzle at the designed printing temperatures to give a print speed of approximately 5 mm/s. The print time of all three drug/polymer tablets was approximability 3 min. The temperature of the build plate was set at 10 °C to prevent the resulting tablets from sticking, thus allow them to be easily removed.

3.3. Characterization of the tablets

All three polymers used in this study are miscible with IBU at the drug level of 40% based on their solubility parameters (δ) (Islam et al., 2015; Maniruzzaman et al., 2015). X-ray powder diffractions analysis was used to evaluate the physical state of IBU within the 3D printed tablets. As shown in Fig. 5a, the XRPD patterns of the pure polymers (EPO, VA64 and SOL) featured broad halos indicating that all three polymers alone were in amorphous state. IBU solid exhibited its crystalline nature with its characteristic diffraction peaks at 5.8°, 12.2°, 16.1°, 17.4°, 18.5°, 20.0° and 22.2°/2θ. As shown in Fig. 5b the characteristic XRPD patterns of IBU were also observed in the physical mixtures (IBU/EPO, IBU/SOL, IBU/VA64), which confirmed that the drug remained as crystalline solid prior to 3D printing.

The characteristic diffraction peaks of IBU were not observed in the XRPD patterns of the 3D printed tablets, which suggested that IBU turned into amorphous state following micro-extrusion (Fig. 5c). XRPD pattern of the 3D printed tablets was also collected a week later. It was confirmed that IBU remained amorphous in the tablets stored at ambient conditions (25 °C, 40% RH) (Supplementary material, Fig. 1).

Thermal analysis was also carried out to investigate the physical state of IBU before and after 3D printing and possible drug-polymer interactions in the printed tablets. The bulk IBU exhibited a melting endotherm at 77.99 °C while SOL, VA 64 and EPO had glass transition (T_g) temperatures at 63.86 °C, 107.10 °C, and 46.99 °C, respectively (Fig. 6). The melting endotherm of IBU was not observed when the printed tablets were heated. As shown in Fig. 7, the IBU/SOL, IBU/VA64 and IBU/EPO thermograms exhibited single glass transitions at 37.69 °C, 77.99 °C and 15.35 °C, respectively. Both observations suggested that crystalline IBU was completely dissolved in the polymers at a drug load of 40% following 3D printing. Amorphous IBU, with a glass transition temperature of −45.15 °C(Dudognon et al., 2008), acted as a plasticizer in the printed tablets and led to lower T_g's [(Gryczke et al., 2011; Islam et al., 2015; Maniruzzaman et al., 2012). Interestingly, the measured glass transition temperatures were higher than the values predicted based on Fox equation. Fox equation has been widely used to estimate the glass transition temperatures of physical mixtures without interaction between the components. This discrepancy suggested strong intramolecular interactions between IBU and the studied polymers.

3.4. Raman spectra and mapping

The interaction between IBU and the polymers were further investigated using Raman spectroscopy. The vibrational bands in the Raman spectra of IBU have been well documented in literature (Breitenbach et al., 1999; Vueba et al., 2008). As shown in Fig. 8, crystalline IBU features hydroxyl methyl and aromatic peaks and more specifically the peak at 637 cm^{-1} represents the out of plane stretching of CO-H bond. Other peaks at 746 cm^{-1}, 850 cm^{-1}, 1609 cm^{-1}, and 3047 cm^{-1} correspond to the out-of-plane deformation of the C-H bonds, the out-of-plane bending the C-H bonds, the stretching of the C-C bonds, and the stretching of the C-H bonds, respectively. In addition, the peaks at 1181 cm^{-1}, 1452 cm^{-1}, and 2965 cm^{-1} are related to the stretching of non-aromatic C-C bond, the asymmetric deformation of CH_3, and the asymmetric stretching of CH_3 bonds, respectively. The same bands were observed in the Raman spectra of the 3D printed IBU/polymer tablets, but with broadened figures comparing to IBU alone.

As shown in Fig. 8, the peaks of C = C vibration of the aryl group in IBU shifted from 1608 cm^{-1} to 1616 cm^{-1} after 3D printed together with the polymers, which suggested a potential H-bond between IBU and the polymers (Hédoux et al., 2011). In addition, the C = O stretching of IBU

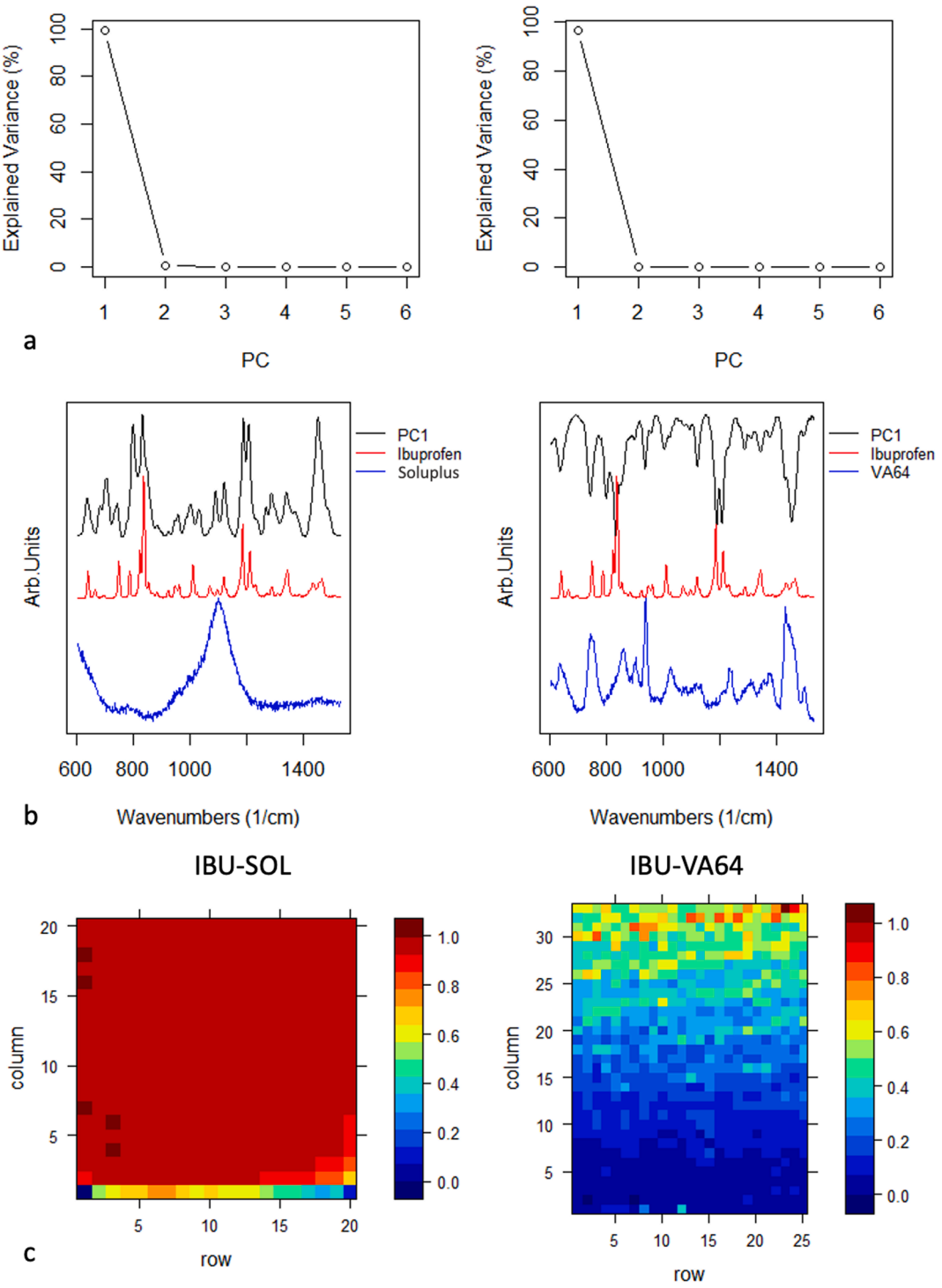

Fig. 9. (a) Explained variance of each PC for IBU-SOL (left) and IBU-VA64 sample, (b) comparison of first PC with the spectra of IBU, SOL and VA64 respectively, and (c) concentration of chemical map for PC1 for IBU-SOL and IBU-VA64.

shifted from 1652 cm^{-1} in the spectra of IBU alone to 1734 cm^{-1} in that of the printed tablets, which is associated to and suggests a strong drug–polymer interaction similar to the one observed for cyclodextrin molecular complexes (Brás et al., 2008). It was also observed that the CO–H out-of-plane bending of the bulk IBU at 637 cm^{-1} and 663 cm^{-1} shifted to 605 cm^{-1} or completely disappeared in the 3D printed tablets (Vueba et al., 2008). This shift suggested a static disorder molecular environment that resulted from the formation of a glass solutions.

In order to investigate the spatial resolution of IBU in the printed tablet the Raman spectra were continuously recorded. PCA has been applied to decompose the spectra into scores and loadings that approximately express the initial spectra. The main advantage of PCA is that it does not require the use of the spectra of bulk compounds which could be undergo changes during print processing due to molecular interactions. The number of principal components needed to decompose the hyperspectral matrix is usually determined by the analysis of eigenvalues which expresses the total variance captured by a specified principal component. In simple systems such as in this case where only two compounds are present with good mixing, two - three PCs are adequate to decompose the system. In more complicated systems the use

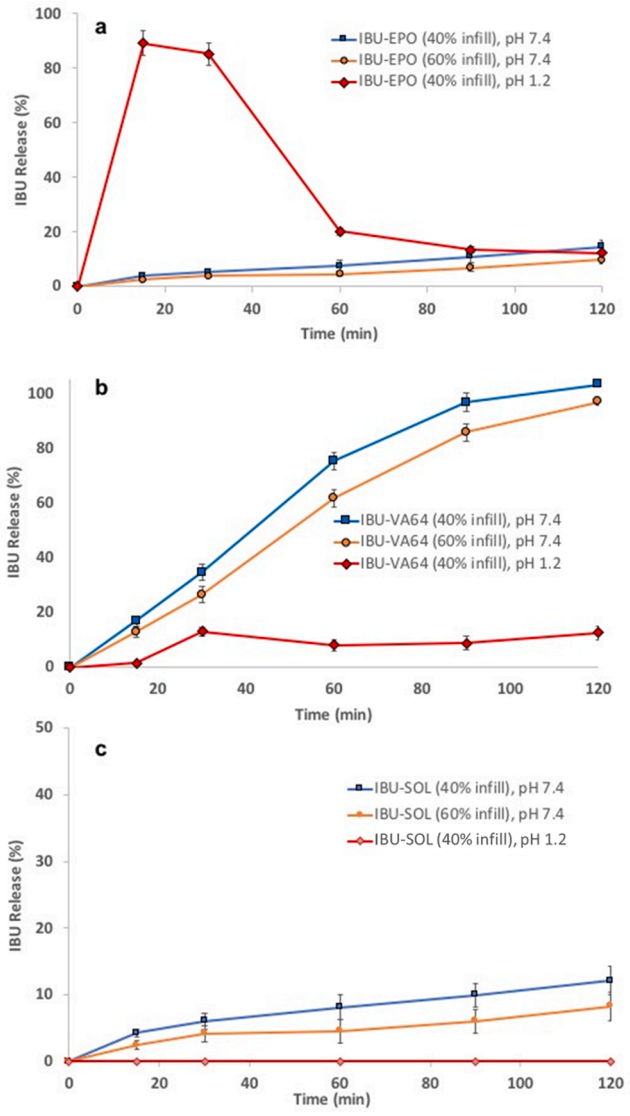

Fig. 10. Dissolution rates of (a) IBU-EPO, (b) IBU-VA64 and (c) IBU-SOL 3D printed tablets with different infill densities at pH 1.2 and pH 7.4 respectively.

of more PCs, where a compound can be identified in a very late component, is not uncommon (Scoutaris et al., 2014). Fig. 9a illustrates the cumulative variance that corresponds to each PC. In the IBU-SOL 3D printed sample the PC (left) expresses 99.4% of the total variance whereas in the of IBU-VA64, the PC (right) covers 96.7% of the total variance. For the former sample the very high variance covered by the PC is due to the very broad peaks of SOL spectrum which cannot be distinguished from that of IBU.

Fig. 9b represents a summary of the PC and the spectra of the tablet's individual components. For the IBU-VA64 sample it is evident that the PC contains peaks corresponding to both components namely the API and the polymer. However, this is not the case for the IBU – SOL samples which couldn't be distinguished due to the presence of its broad peak. As shown in Fig. 9c the plotting of the concentration map for the first PC of the IBU-SOL and the IBU- VA64 demonstrates that the compounds are homogeneously distributed within the tablet. This is a proof of strong drug-polymer intermolecular interactions and that the IBU is molecularly dispersed within the polymer matrix.

3.5. Dissolution studies

Drug release may be modified by dispersing the drug into a polymeric matrix at molecular level following 3D printing of a drug/polymer blend (Douroumis et al., 2007; Islam et al., 2015; Maniruzzaman et al., 2015). The dissolutions of IBU from the 3D printed tablets were evaluated in both acidic (pH 1.2) and alkaline media (pH 7.4) and revealed the impact of polymer type as well as the infill density (40% and 60%) on the drug release from the tablets.

Eudragit EPO is a basic methacrylate copolymer that has been commonly used in immediate release drug product requiring taste masking because it is practically insoluble at pH greater than 5 (in saliva), while highly soluble in acidic media (in stomach). As expected, IBU/EPO tablets exhibited a slow dissolution at pH 7.4, despite IBU was dispersed in the polymer matrix at the molecular level (Fine-Shamir and Dahan, 2019; Gryczke et al., 2011). The tablet with 40% infill density showed an ~15% drug release in 2 h, while the tablet with 60% infill density presented an ~10% drug release in the same period (Fig. 10a). A slightly higher drug release from the tablet with lower fill density was attributed to larger surface of the tablet. The IBU/EPO tablets had a rapid dissolution at pH 1.2 with ~89% drug released within 15 min and generated a high degree of supersaturation. As EPO was not a good crystallization inhibitor the concentration of IBU in the dissolution media dropped significantly following the initial drug release due to the

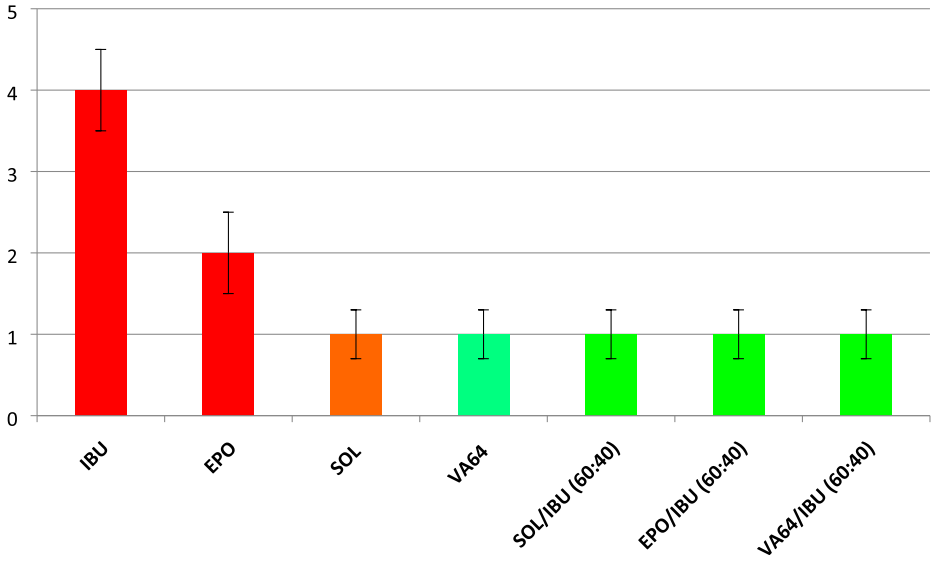

Fig. 11. Taste mask evaluation of IBU, EPO, SOL, VA64 and 3D printed VA64/IBU, SOL/IBU and EPO/IBU tablets.

crystallization of IBU.

PVP-VA64 is a neutral vinylpyrrolidone-vinyl acetate copolymer with good solubility in water across large pH range. IBU is an acidic compound (pKa 4.6), which has a low solubility at low pH. The release of IBU from the 3D printed IBU/VA64 tablets were found low at pH 1.2 with an ~13% drug release in 2 h (Fig. 10b). The slow release of IBU from VA64 matrix with high drug load at low pH $\leq$ 2 was also observed previously (Tres et al., 2016). The authors concluded that VA64 dissolved preferentially from the exterior of the printed tablet (compact) that resulted in an amorphous IBU-rich and hydrophobic shell. The hydrophobic shell acted as in situ enteric coating and inhibits the dissolution. At pH 7.4, the solubility of IBU was significantly higher, which had IBU released at a similar rate as polymer. The congruency of IBU and polymer generated a supersaturation of IBU. In addition, PVP-VA64 inhibited the crystallization of IBU in the solution, which maintained the level of supersaturation throughout the dissolution test. The IBU-VA64 tablet with 40% fill density showed a slightly higher dissolution rate than the tablet with 60% fill density. This comparison again confirmed that greater tablet surface resulted in higher drug release.

Soluplus is a well-known polymeric solubilizer that was found to facilitate drug release in several occasions due to the enhanced drug-polymer interactions. However, as shown in Fig. 10c, all IBU-SOL tablets exhibited slow dissolution at both pH 1.2 and 7.4. Pudlas et al, had a similar observation for IBU-SOL extrudates and investigated the root cause using spectroscopic analysis. The slow release of IBU was attributed to the strong H-bonding between IBU and VA64 which consumed large number of hydrophilic groups in the polymer chain thus significantly reduced the hydrophilicity of the polymer. Further evidence was provided by Walsh et al. (2018) who observed that SOL exhibits a lower critical solution temperature at 40 °C and the chins lose hydration leading to the formation of a cloudy suspension with reduced solubility (Walsh et al., 2018) [x]. As a result, a gel formation takes place with reduced IBU dissolution rates due to the SOL properties (Fini, 2016). Comparatively, the drug release at pH 1.2 was slowest due to the low solubility of IBU at acidic conditions. The impact of infill density on the drug release was again observed, i.e., the IBU/Sol tablet with 40% fill density gave slightly faster dissolution than that with 60% fill density.

Overall, the tablets with lower infill density gave a higher dissolution rate due to higher surface area. The impact of polymer on the dissolution of the IBU/polymer tablets depends on the characteristics of the compound, polymers, as well as their interactions.

3.6. Taste masking evaluation

A drug product for paediatric use is governed by stricter regulations introduced by the European Medicines Agency (EMEA, 2007). Strickley et al. (2008) identified challenges in paediatric product development associated to dose flexibility and taste masking.

IBU is known to have a bitter or salty taste and thus taste masking is required in the finished product consisting IBU for paediatric use. As shown in Fig. 11, the taste of IBU and the 3D printed IBU/polymer tablets were assessed in healthy panellists. IBU had an average score of 4, which confirmed the bitterness taste of the drug while the bulk polymers had acceptable taste with bitterness scores of 2 or below. All 3D printed IBU/polymer tablets had pleasant taste with bitterness score of 1. As previously reported the effective taste masking of bitter APIs is directly related to the H-bonding interactions between the drug and polymer carriers (Gryczke et al., 2011, Maniruzzaman et al., 2012). The effective taste masking of IBU in the chewable tablets demonstrated that micro-extrusion can be successfully used for 3D printing of personalized tablets for paediatric use.

4. Conclusions

In this study we demonstrated a simple micro-extrusion 3D printing technique that can be used to 3D print tablets with suitable and reproducible printability. Such 3D printing technology can bypass the pre- and post-processing procedures that other 3D printing technologies require. In addition, such an approach minimises material wastes compared to other 3D printing technologies. Similar to other 3D printing technology, micro-extrusion 3D printing can also be used to fabricate drug products with specific release profile tailored to individual patient by selecting suitable polymer matrix and modifying infill density of the tablets.

CRediT authorship contribution statement

Atabak Ghanizadeh Tabriz: Writing – original draft. **Uttom Nandi:** Writing – original draft. **Nicolaos Scoutaris:** Writing – original draft. **Karifa Sanfo:** Writing – original draft. **Bruce Alexander:** Writing – original draft. **Yuchuan Gong:** Conceptualization, Project administration, Supervision, Writing – review & editing, Funding acquisition. **Ho-Wah Hui:** Conceptualization, Project administration, Supervision, Writing – review & editing, Funding acquisition. **Sumit Kumar:** Conceptualization, Project administration, Supervision, Writing – review & editing, Funding acquisition. **Dennis Douroumis:** Conceptualization, Project administration, Supervision, Writing – review & editing, Funding acquisition.

Declaration of Competing Interest

The authors declare that they have no known competing financial interests or personal relationships that could have appeared to influence the work reported in this paper.

References

Alhijjaj, M., Belton, P., Qi, S., 2016. An investigation into the use of polymer blends to improve the printability of and regulate drug release from pharmaceutical solid dispersions prepared via fused deposition modeling (FDM) 3D printing. Eur. J. Pharm. Biopharm. 108, 111–125. https://doi.org/10.1016/j.ejpb.2016.08.016.

Barbero, N., Barolo, C., Viscardi, G., 2016. Bovine serum albumin bioconjugation with FITC. World J. Chem. Educ. 4, 80–85. https://doi.org/10.12691/wjce-4-4-3.

Boniatti, J., Januskaite, P., Fonseca, L.B.d., Viçosa, A.L., Amendoeira, F.C., Tuleu, C., Basit, A.W., Goyanes, A., Ré, M.-I., 2021. Direct powder extrusion 3d printing of praziquantel to overcome neglected disease formulation challenges in paediatric populations. Pharmaceutics 13 (8), 1114.

Brás, A.R., Noronha, J.P., Antunes, A.M.M., Cardoso, M.M., Schönhals, A., Affouard, F., Dionísio, M., Correia, N.T., 2008. Molecular motions in amorphous ibuprofen as studied by broadband dielectric spectroscopy. J. Phys. Chem. B 112, 11087–11099. https://doi.org/10.1021/jp8040428.

Breitenbach, J., Schrof, W., Neumann, J., 1999. Confocal Raman-spectroscopy: analytical approach to solid dispersions and mapping of drugs. Pharm. Res. 16, 1109–1113. https://doi.org/10.1023/A:1018956304595.

Castellano, J.M., Sanz, G., Peñalvo, J.L., Bansilal, S., Fernández-Ortiz, A., Alvarez, L., Guzmán, L., Linares, J.C., García, F., D'Aniello, F., Arnáiz, J.A., Varea, S., Martínez, F., Lorenzatti, A., Imaz, I., Sánchez-Gómez, L.M., Roncaglioni, M.C., Baviera, M., Smith, S.C., Taubert, K., Pocock, S., Brotons, C., Farkouh, M.E., Fuster, V., 2014. A polypill strategy to improve adherence: results from the FOCUS project. J. Am. Coll. Cardiol. 64, 2071–2082. https://doi.org/10.1016/j.jacc.2014.08.021.

Chai, X., Chai, H., Wang, X., Yang, J., Li, J., Zhao, Y., Cai, W., Tao, T., Xiang, X., 2017. Fused Deposition Modeling (FDM) 3D printed tablets for intragastric floating delivery of domperidone. Sci. Rep. 7, 2829. https://doi.org/10.1038/s41598-017-03097-x.

Douroumis, D., Bouropoulos, N., Fahr, A., 2007. Physicochemical characterization of solid dispersions of three antiepileptic drugs prepared by solvent evaporation method. J. Pharm. Pharmacol. 59, 645–653. https://doi.org/10.1211/jpp.59.5.0004.

Dudognon, E., Danède, F., Descamps, M., Correia, N.T., 2008. Evidence for a new crystalline phase of racemic ibuprofen. Pharm. Res. 25, 2853–2858. https://doi.org/10.1007/s11095-008-9655-7.

Eilers, P.H.C., Boelens, H.F.M., 2005. Baseline correction with asymmetric least squares smoothing. Life Sci.

Elbadawi, M., Gustaffson, T., Gaisford, S., Basit, A.W., 2020. 3D printing tablets: Predicting printability and drug dissolution from rheological data. Int. J. Pharm. 590, 119868. https://doi.org/10.1016/j.ijpharm.2020.119868.

Fina, F., Goyanes, A., Gaisford, S., Basit, A.W., 2017. Selective laser sintering (SLS) 3D printing of medicines. Int. J. Pharm. 529, 285–293. https://doi.org/10.1016/j.ijpharm.2017.06.082.

Fina, F., Goyanes, A., Madla, C.M., Awad, A., Trenfield, S.J., Kuek, J.M., Patel, P., Gaisford, S., Basit, A.W., 2018. 3D printing of drug-loaded gyroid lattices using

selective laser sintering. Int. J. Pharm. 547, 44–52. https://doi.org/10.1016/j.ijpharm.2018.05.044.
Fine-Shamir, N., Dahan, A., 2019. Methacrylate-copolymer eudragit EPO as a solubility-enabling excipient for anionic drugs: investigation of drug solubility, intestinal permeability, and their interplay. Mol. Pharm. 16, 2884–2891. https://doi.org/10.1021/acs.molpharmaceut.9b00057.
Fini, A., 2016. Release Problems for Nifedipine in the Presence of Soluplus. J. Pharm. Pharm. <https://doi.org/10.15436/2377-1313.16.020>.
Fuenmayor, E., Forde, M., Healy, A., Devine, D., Lyons, J., McConville, C., Major, I., 2018. Material considerations for fused-filament fabrication of solid dosage forms. Pharmaceutics 10 (2), 44.
Ghanizadeh Tabriz, A., Nandi, U., Hurt, A.P., Hui, H.-W., Karki, S., Gong, Y., Kumar, S., Douroumis, D., 2020. 3D printed bilayer tablet with dual controlled drug release for tuberculosis treatment. Int. J. Pharm. 120147 https://doi.org/10.1016/j.ijpharm.2020.120147.
Gioumouxouzis, C.I., Baklavaridis, A., Katsamenis, O.L., Markopoulou, C.K., Bouropoulos, N., Tzetzis, D., Fatouros, D.G., 2018. A 3D printed bilayer oral solid dosage form combining metformin for prolonged and glimepiride for immediate drug delivery. Eur. J. Pharm. Sci. 120, 40–52. https://doi.org/10.1016/j.ejps.2018.04.020.
Goyanes, A., Allahham, N., Trenfield, S.J., Stoyanov, E., Gaisford, S., Basit, A.W., 2019. Direct powder extrusion 3D printing: Fabrication of drug products using a novel single-step process. Int. J. Pharm. 567, 118471.
Goyanes, A., Buanz, A.B.M., Hatton, G.B., Gaisford, S., Basit, A.W., 2015a. 3D printing of modified-release aminosalicylate (4-ASA and 5-ASA) tablets. Eur. J. Pharm. Biopharm. 89, 157–162. https://doi.org/10.1016/j.ejpb.2014.12.003.
Goyanes, A., Fina, F., Martorana, A., Sedough, D., Gaisford, S., Basit, A.W., 2017. Development of modified release 3D printed tablets (printlets) with pharmaceutical excipients using additive manufacturing. Int. J. Pharm. 527, 21–30. https://doi.org/10.1016/j.ijpharm.2017.05.021.
Goyanes, A., Wang, J., Buanz, A., Martínez-Pacheco, R., Telford, R., Gaisford, S., Basit, A.W., 2015b. 3D printing of medicines: engineering novel oral devices with unique design and drug release characteristics. Mol. Pharm. 12, 4077–4084. https://doi.org/10.1021/acs.molpharmaceut.5b00510.
Gryczke, A., Schminke, S., Maniruzzaman, M., Beck, J., Douroumis, D., 2011. Development and evaluation of orally disintegrating tablets (ODTs) containing Ibuprofen granules prepared by hot melt extrusion. Colloids Surf. B. Biointerf. 86, 275–284. https://doi.org/10.1016/j.colsurfb.2011.04.007.
Hafezi, F., Scoutaris, N., Douroumis, D., Boateng, J., 2019. 3D printed chitosan dressing crosslinked with genipin for potential healing of chronic wounds. Int. J. Pharm. 560, 406–415. https://doi.org/10.1016/j.ijpharm.2019.02.020.
Hédoux, A., Guinet, Y., Derollez, P., Dudognon, E., Correia, N.T., 2011. Raman spectroscopy of racemic ibuprofen: evidence of molecular disorder in phase II. Int. J. Pharm. 421, 45–52. https://doi.org/10.1016/j.ijpharm.2011.09.015.
Islam, M.T., Scoutaris, N., Maniruzzaman, M., Moradiya, H.G., Halsey, S.A., Bradley, M. S.A., Chowdhry, B.Z., Snowden, M.J., Douroumis, D., 2015. Implementation of transmission NIR as a PAT tool for monitoring drug transformation during HME processing. Eur. J. Pharm. Biopharm. Off. J. Arbeitsgemeinschaft. Pharm. Verfahrenstechnik e.V 96, 106–116. https://doi.org/10.1016/j.ejpb.2015.06.021.
Jamróz, W., Kurek, M., Czech, A., Szafraniec, J., Gawlak, K., Jachowicz, R., 2018. 3D printing of tablets containing amorphous aripiprazole by filaments co-extrusion. Eur. J. Pharm. Biopharm. 131, 44–47. https://doi.org/10.1016/j.ejpb.2018.07.017.
Januskaite, P., Xu, X., Ranmal, S.R., Gaisford, S., Basit, A.W., Tuleu, C., Goyanes, A., 2020. I spy with my little eye: a paediatric visual preferences survey of 3D printed tablets. Pharmaceutics 12 (11), 1100.
Kadry, H., Al-Hilal, T.A., Keshavarz, A., Alam, F., Xu, C., Joy, A., Ahsan, F., 2018. Multi-purposable filaments of HPMC for 3D printing of medications with tailored drug release and timed-absorption. Int. J. Pharm. 544, 285–296. https://doi.org/10.1016/J.IJPHARM.2018.04.010.
Kyobula, M., Adedeji, A., Alexander, M.R., Saleh, E., Wildman, R., Ashcroft, I., Gellert, P. R., Roberts, C.J., 2017. 3D inkjet printing of tablets exploiting bespoke complex geometries for controlled and tuneable drug release. J. Control. Release 261, 207–215. https://doi.org/10.1016/j.jconrel.2017.06.025.
Maniruzzaman, M., Boateng, J.S., Bonnefille, M., Aranyos, A., Mitchell, J.C., Douroumis, D., 2012. Taste masking of paracetamol by hot-melt extrusion: an in vitro and in vivo evaluation. Eur. J. Pharm. Biopharm. 80, 433–442. https://doi.org/10.1016/j.ejpb.2011.10.019.
Maniruzzaman, M., Pang, J., Morgan, D.J., Douroumis, D., 2015. Molecular modeling as a predictive tool for the development of solid dispersions. Mol. Pharm. 12, 1040–1049. https://doi.org/10.1021/mp500510m.
Martinez, P.R., Goyanes, A., Basit, A.W., Gaisford, S., 2018. Influence of geometry on the drug release profiles of stereolithographic (SLA) 3D-printed tablets. AAPS PharmSciTech 19, 3355–3361. https://doi.org/10.1208/s12249-018-1075-3.
Nasereddin, J.M., Wellner, N., Alhijjaj, M., Belton, P., Qi, S., 2018. Development of a simple mechanical screening method for predicting the feedability of a pharmaceutical FDM 3D printing filament. Pharm. Res. 35, 151. https://doi.org/10.1007/s11095-018-2432-3.
Öblom, H., Zhang, J., Pimparade, M., Speer, I., Preis, M., Repka, M., Sandler, N., 2019. 3D-printed isoniazid tablets for the treatment and prevention of tuberculosis—personalized dosing and drug release. AAPS PharmSciTech 20, 52. https://doi.org/10.1208/s12249-018-1233-7.
Pere, C.P.P., Economidou, S.N., Lall, G., Ziraud, C., Boateng, J.S., Alexander, B.D., Lamprou, D.A., Douroumis, D., 2018. 3D printed microneedles for insulin skin delivery. Int. J. Pharm. 544, 425–432. https://doi.org/10.1016/j.ijpharm.2018.03.031.
Pereira, B.C., Isreb, A., Forbes, R.T., Dores, F., Habashy, R., Petit, J.-B., Alhnan, M.A., Oga, E.F., 2019. 'Temporary Plasticiser': a novel solution to fabricate 3D printed patient-centred cardiovascular 'Polypill' architectures. Eur. J. Pharm. Biopharm. 135, 94–103. https://doi.org/10.1016/j.ejpb.2018.12.009.
R Core Team, 2019. R: A language and environment for statistical computing. R Found. Stat. Comput.
Rycerz, K., Stepien, K.A., Czapiewska, M., Arafat, B.T., Habashy, R., Isreb, A., Peak, M., Alhnan, M.A., 2019. Embedded 3D printing of novel bespoke soft dosage form concept for pediatrics. Pharmaceutics 11, 630. https://doi.org/10.3390/pharmaceutics11120630.
Sadia, M., Sośnicka, A., Arafat, B., Isreb, A., Ahmed, W., Kelarakis, A., Alhnan, M.A., 2016. Adaptation of pharmaceutical excipients to FDM 3D printing for the fabrication of patient-tailored immediate release tablets. Int. J. Pharm. 513, 659–668. https://doi.org/10.1016/j.ijpharm.2016.09.050.
Scoutaris, N., Vithani, K., Slipper, I., Chowdhry, B., Douroumis, D., 2014. SEM/EDX and confocal Raman microscopy as complementary tools for the characterization of pharmaceutical tablets. Int. J. Pharm. 470, 88–98. https://doi.org/10.1016/j.ijpharm.2014.05.007.
Scoutaris, N., Ross, S., Douroumis, D., 2016. Current trends on medical and pharmaceutical applications of inkjet printing technology. Pharm. Res. 33, 1799–1816. https://doi.org/10.1007/s11095-016-1931-3.
Scoutaris, N., Ross, S.A., Douroumis, D., 2018. 3D printed "Starmix" drug loaded dosage forms for paediatric applications. Pharm. Res. 35, 34. https://doi.org/10.1007/s11095-017-2284-2.
Strickley, R.G., Iwata, Q., Wu, S., Dahl, T.C., 2008. Pediatric drugs–a review of commercially available oral formulations. J. Pharm. Sci. 97, 1731–1774. https://doi.org/10.1002/jps.21101.
Tagami, T., Ito, E., Kida, R., Hirose, K., Noda, T., Ozeki, T., 2021. 3D printing of gummy drug formulations composed of gelatin and an HPMC-based hydrogel for pediatric use. Int. J. Pharm. 594, 120118. https://doi.org/10.1016/j.ijpharm.2020.120118.
Trenfield, S.J., Awad, A., Goyanes, A., Gaisford, S., Basit, A.W., 2018. 3D printing pharmaceuticals: drug development to frontline care. Trends Pharmacol. Sci. 39, 440–451. https://doi.org/10.1016/j.tips.2018.02.006.
Tres, F., Treacher, K., Booth, J., Hughes, L.P., Wren, S.A.C., Aylott, J.W., Burley, J.C., 2016. Indomethacin-kollidon VA64 extrudates: a mechanistic study of pH-dependent controlled release. Mol. Pharm. 13, 1166–1175. https://doi.org/10.1021/acs.molpharmaceut.5b00979.
Vueba, M.L., Pina, M.E., Batista de Carvalho, L.A.E., 2008. Conformational stability of ibuprofen: assessed by DFT calculations and optical vibrational spectroscopy. J. Pharm. Sci. 97, 845–859. https://doi.org/10.1002/jps.21007.
Walsh, D., Serrano, D.R., Worku, Z.A., Madi, A.M., O'Connell, P., Twamley, B., Healy, A. M., 2018. Engineering of pharmaceutical cocrystals in an excipient matrix: spray drying versus hot melt extrusion. Int. J. Pharm. 551 (1–2), 241–256.
Wang, H., Dumpa, N., Bandari, S., Durig, T., Repka, M.A., 2020. Fabrication of taste-masked donut-shaped tablets via fused filament fabrication 3D printing paired with hot-melt extrusion techniques. AAPS PharmSciTech 21, 243. https://doi.org/10.1208/s12249-020-01783-0.
Wang, J., Goyanes, A., Gaisford, S., Basit, A.W., 2016. Stereolithographic (SLA) 3D printing of oral modified-release dosage forms. Int. J. Pharm. 503, 207–212. https://doi.org/10.1016/j.ijpharm.2016.03.016.
Wehrens, R., Bloemberg, T.G., Eilers, P.H.C., 2015. Fast parametric time warping of peak lists. Bioinformatics. https://doi.org/10.1093/bioinformatics/btv299.
Xu, P., Li, J., Meda, A., Osei-Yeboah, F., Peterson, M.L., Repka, M., Zhan, X., 2020. Development of a quantitative method to evaluate the printability of filaments for fused deposition modeling 3D printing. Int. J. Pharm. 588, 119760. https://doi.org/10.1016/j.ijpharm.2020.119760.
Yang, Y., Wang, H., Li, H., Ou, Z., Yang, G., 2018. 3D printed tablets with internal scaffold structure using ethyl cellulose to achieve sustained ibuprofen release. Eur. J. Pharm. Sci. 115, 11–18. https://doi.org/10.1016/j.ejps.2018.01.005.
Zhang, J., Feng, X., Patil, H., Tiwari, R.V., Repka, M.A., 2017. Coupling 3D printing with hot-melt extrusion to produce controlled-release tablets. Int. J. Pharm. 519, 186–197. https://doi.org/10.1016/j.ijpharm.2016.12.049.
Zhu, X., Li, H., Huang, L., Zhang, M., Fan, W., Cui, L., 2020. 3D printing promotes the development of drugs. Biomed. Pharmacother. 131, 110644. https://doi.org/10.1016/j.biopha.2020.110644.